SUPPLEMENTARY INFORMATION

A lactate-dependent shift of glycolysis mediates synaptic and cognitive processes in male mice

Ignacio Fernández-Moncada[1]*, Gianluca Lavanco[1,2,16,17], Unai B. Fundazuri[1,17], Nasrin Bollmohr[1,17], Sarah Mountadem[1,17], Tommaso Dalla Tor[1,2,17], Pauline Hachaguer[1], Francisca Julio-Kalajzic[1], Doriane Gisquet[1], , Roman Serrat[1,3], Luigi Bellocchio[1], Astrid Cannich[1], Bérénice Fortunato-Marsol[1], Yusuke Nasu[4,5], Robert E. Campbell[4,6], Filippo Drago[2], Carla Cannizzaro[7], Guillaume Ferreira[3], Anne-Karine Bouzier-Sore[8], Luc Pellerin[9], Juan P. Bolaños[10,11,12], Gilles Bonvento[13], L. Felipe Barros[14,15], Stephane H. R. Oliet[1], Aude Panatier[1,18], Giovanni Marsicano[1,18,*]

[1]Univ. Bordeaux, INSERM, Neurocentre Magendie, U1215, F-33000 Bordeaux, France.

[2]Department of Biomedical and Biotechnological Sciences, Section of Pharmacology, University of Catania, Catania 95124, Italy.

[3]University of Bordeaux, INRAE, Bordeaux INP, NutriNeurO, UMR 1286, Bordeaux, France.

[4]Department of Chemistry, School of Science, The University of Tokyo, Bunkyo-ku, Tokyo 113-0033, Japan.

[5]PRESTO, Japan Science and Technology Agency, Chiyoda-ku, Tokyo 102-0075, Japan.

[6]Université Laval, CERVO Brain Research Center and Department of Biochemistry, Microbiology, and Bioinformatics, Québec, Québec, Canada.

[7]Department of Biomedicine, Neuroscience and Advanced Diagnostics, University of Palermo, Italy.

[8]Université de Bordeaux, CNRS, Centre de Résonance Magnétique des Systèmes Biologiques, UMR 5536, F-33000 Bordeaux, France.

[9]Université de Poitiers et CHU de Poitiers, INSERM, IRMETIST, U1313, Poitiers, France.

[10]Institute of Functional Biology and Genomics (IBFG), Universidad de Salamanca, CSIC, Salamanca, Spain.

[11]Institute of Biomedical Research of Salamanca (IBSAL), Hospital Universitario de Salamanca, Salamanca, Spain.

[12]Centro de Investigación Biomédica en Red de Fragilidad y Envejecimiento Saludable (CIBERFES), Madrid, Spain.

[13]Universite Paris-Saclay, CEA, CNRS, MIRCen, Laboratoire des Maladies Neurodegeneratives, Fontenay-aux-Roses, France.

[14]Centro de Estudios Cientificos, Valdivia, Chile.

[15]Universidad San Sebastián, Facultad de Medicina y Ciencia, Valdivia, Chile.

[16]Current address: Department of Health Promotion, Mother and Child Care, Internal Medicine and Medical Specialties, ‘’G. D’Alessandro’’, University of Palermo. Palermo 90127, Italy.

[17]These authors contributed equally.

[18]These authors jointly supervised this work.

*Correspondence:

giovanni.marsicano@inserm.fr (G.M.)

ignacio.fernandez-moncada@inserm.fr (I.F-M.)

Inventory of Supporting Information

Supplementary Fig. 1 – Differential effect of cannabinoids on astrocyte lactate level.

Supplementary Fig. 2 – The basal lactate level and accumulation upon mitochondria inhibition is not altered by CB1 receptor subcellular localization.

Supplementary Fig. 3 – Activation of astroglial CB1 receptors increases lactate production.

Supplementary Fig. 4 – The PKC signaling controls the CB1 receptor-mediated intracellular lactate increase.

Supplementary Fig. 5 – The mitochondrial localization of CB1 receptors is not necessary for physiological novel object exploration.

Supplementary Fig. 6 – Inhibition of the phosphorylated pathway impairs long-term NOR memory in WT mice and in lactate-treated GFAP-CB1-KO mice.

Supplementary Fig. 7 – Activation of HCA1R promotes a biased glucose metabolism.

Supplementary Fig. 8 – Lactate requires the phosphorylated pathway to potentiate NMDAR function.

Supplementary Fig. 9 – Lactate rescues the THC-mediated impairment in novel object exploration via HCAR1 signaling and L-serine production.

Supplementary Fig. 10 – A lactate-dependent shift of glycolysis mediates synaptic and cognitive processes.

Supplementary Table 1 – Details of the double-viral rescue approach to study mtCB1 receptor involvement in NOR performance

Supplementary Table 2 – Statistics details of Main Figures.

Supplementary Table 3 – Statistics details of Supplementary Figures.

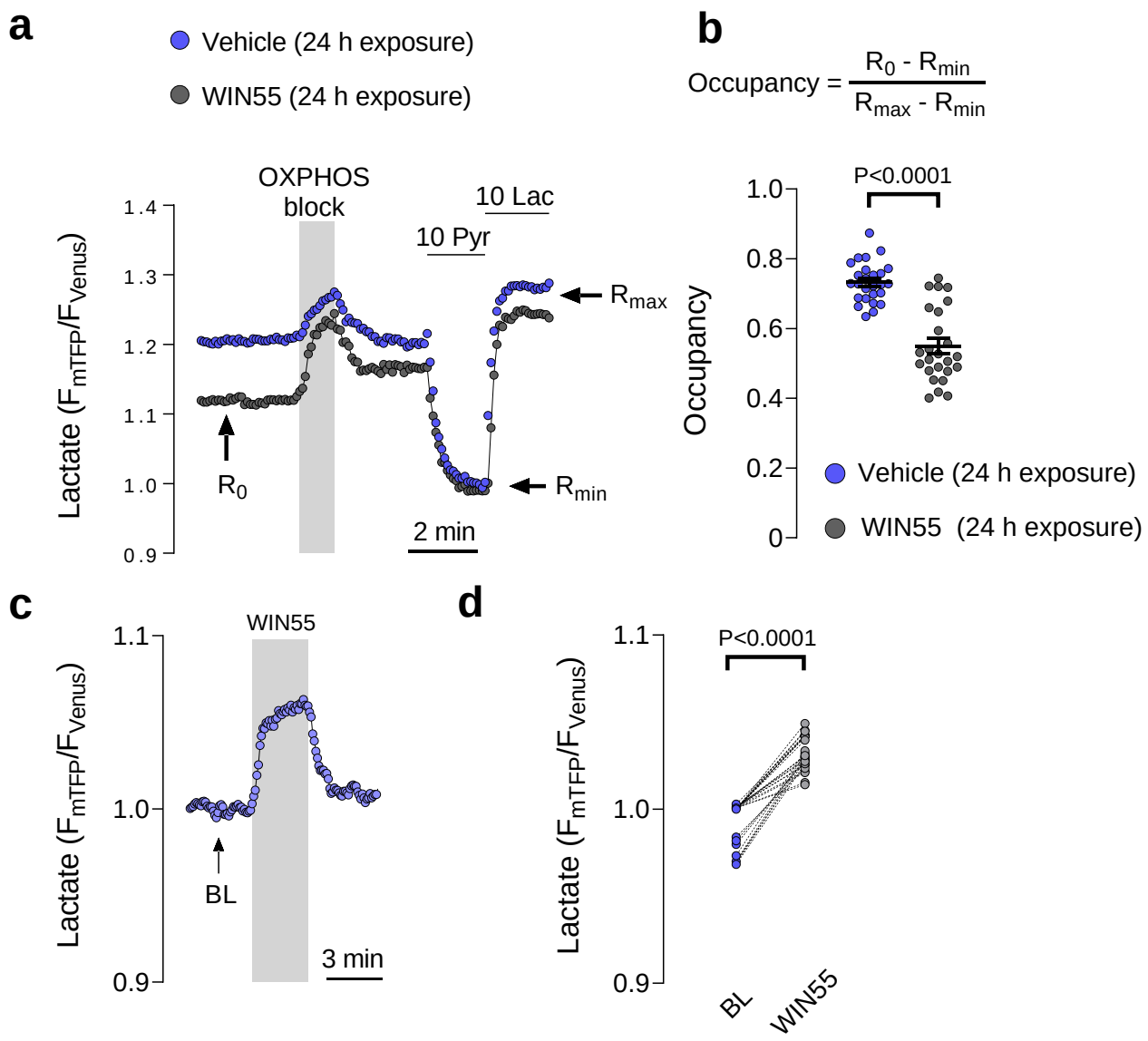

Supplementary Figure 1 – Differential effect of cannabinoids on astrocyte lactate level. a, Intracellular lactate imaging in astrocytes previously incubated with WIN55 (2 μM) or vehicle (DMSO) for 24 hours. After treatment, and to determine the basal lactate level (occupancy), cells were imaged and exposed sequentially to an OXPHOS blocker (5 mM sodium azide), pyruvate (10 mM) and lactate (10 mM). R_0, basal ratio. R_{min}, minimum ratio. R_{max}, maximum ratio. Data was normalized to R_{min} to emphasize the difference in R_0. **b**, Basal lactate level (occupancy) after 24 hours treatment with WIN55 (2 μM) or vehicle (DMSO). Data was computed as occupancy = $(R_0-R_{min})/(R_{max}-R_{min})$, using R_0, R_{min} and R_{max} from experiments similar to panel A. Vehicle, n=3, 26 cells. WIN55, n=3, 25 cells. **c**, Intracellular lactate imaging in astrocytes acutely exposed to WIN55 (2 μM). BL = baseline. **d**, Summary of intracellular lactate level at baseline (BL) and after 3 min exposure to WIN55 (2 μM), in experiments similar to Supplementary Fig. 1C, n=3, 26 cells. Data correspond to representative cells (**a**,**c**). Circles in scatter and before-after plots correspond to single cells (**b**,**d**). Statistical analysis was performed using a two-tailed unpaired t-test (**b**) and two-tailed paired t-test (**d**). See Supplementary Table 3 for more details. Source data are provided as a Source Data file.

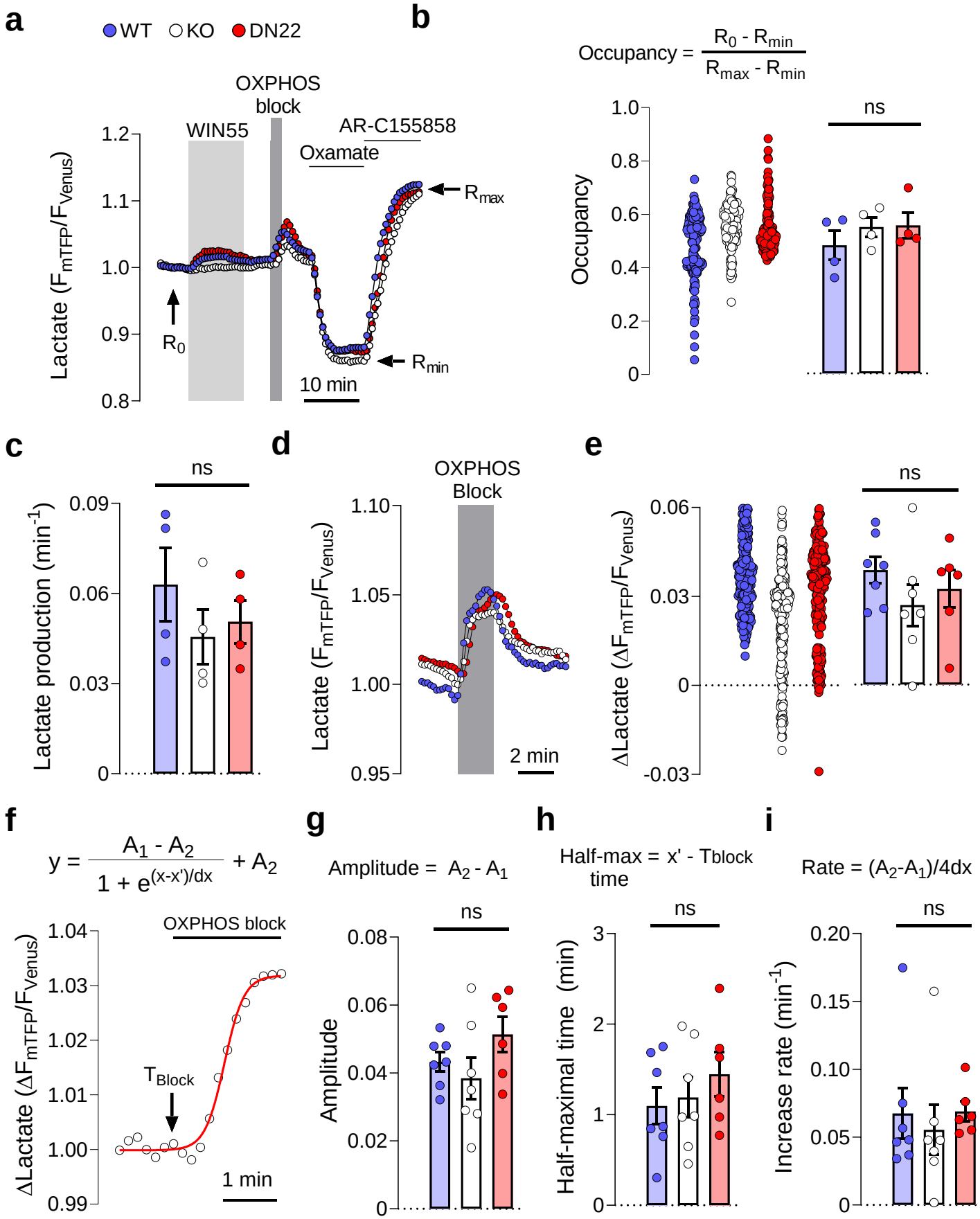
a
WT
KO
DN22
OXPHOS block
WIN55
AR-C155858
Oxamate
Rmax
R0
Rmin
10 min
Lactate (FmTFP/FVenus)
b
Occupancy = (R0 - Rmin) / (Rmax - Rmin)
Occupancy
ns
c
ns
Lactate production (min-1)
d
OXPHOS Block
Lactate (FmTFP/FVenus)
2 min
e
ns
ΔLactate (ΔFmTFP/FVenus)
f
y = (A1 - A2) / (1 + e(x-x')/dx) + A2
OXPHOS block
TBlock
1 min
ΔLactate (ΔFmTFP/FVenus)
g
Amplitude = A2 - A1
ns
Amplitude
h
Half-max = x' - Tblock time
ns
Half-maximal time (min)
i
Rate = (A2-A1)/4dx
ns
Increase rate (min-1)

Supplementary Figure 2 – The basal lactate level and accumulation upon mitochondria inhibition is not altered by CB1 receptor subcellular localization. a, Intracellular lactate imaging in astrocytes. To determine the basal lactate level (occupancy), cells exposed sequentially to WIN55 (1 μM), OXPHOS block (5 mM azide), Oxamate (6 mM) and AR-C155858 (1 μM). R_0, basal ratio. R_{min}, minimum ratio. R_{max}, maximum ratio. Average of 4 independent experiments. Cells: WT=158, KO=145, DN22=154. **b**, Basal lactate level (occupancy) in CB1-WT, CB1-KO and DN22-CB1-KI astrocytes. Data was computed as occupancy = $(R_0-R_{min})/(R_{max}-R_{min})$, using R_0, R_{min} and R_{max} obtained from experiments similar to panel A. N = 4, cells analyzed: CB1-WT=158, CB1-KO=145, DN22-CB1-KI =154. **c,** Basal lactate production rates in WT, KO and DN22 astrocytes. N=4 **d**, Intracellular lactate accumulation induced by OXPHOS block (5 mM sodium azide). Average of several cells in a representative experiment (CB1-WT=32, CB1-KO=48, DN22-CB1-KI =36 cells). **e**, Summary of intracellular lactate levels after 2 min of OXPHOS block (5 mM sodium azide), in experiments similar to those shown in panel C. CB1-WT: n=7, 247 cells. CB1-KO: n=7, 227 cells. DN22-CB1-KI: n=6, 205 cells. **f**, Representative non-linear fitting of a sigmoidal model (Boltzmann equation, on top) to the lactate increase induced by OXPHOS blocking. The fitted parameters A_1, A_2, x' and dx were used to compute the amplitude, half-maximal time and increase rate presented in panel G-I. T_{block}, time of exposure to OXPHOS blocker sodium azide. **g**, Amplitude of lactate changes induced by OXPHOS block obtained from a non-linear fitting data. CB1-WT: n=7; CB1-KO: n=7; DN22-CB1-KI: n=6. **h**, Half-maximal time of lactate changes induced by OXPHOS block obtained from a non-linear fitting data. CB1-WT: n=7; CB1-KO: n=7; DN22-CB1-KI: n=6. **I**, Half-maximal time of lactate changes induced by OXPHOS block obtained from a non-linear fitting data. CB1-WT: n=7; CB1-KO: n=7; DN22-CB1-KI: n=6. Data corresponds to the experiments average and represented as mean±SEM (**a**,**d**). Circles in scatter plots correspond to single cells (**b**,**e**). Bars correspond to experiments average (mean±SEM) and circles represent individual experiment average (**b**,**c**,**e**,**g**,**h**,**i**). Statistical analysis was performed using Kruskal-Wallis test followed by Dunn's multiple comparison test (**b**), One-way ANOVA followed by Tukey's multiple comparison test (**c**,**e**,**g**,**h**,**i**). See Supplementary Table 3 for more details. Source data are provided as a Source Data file.

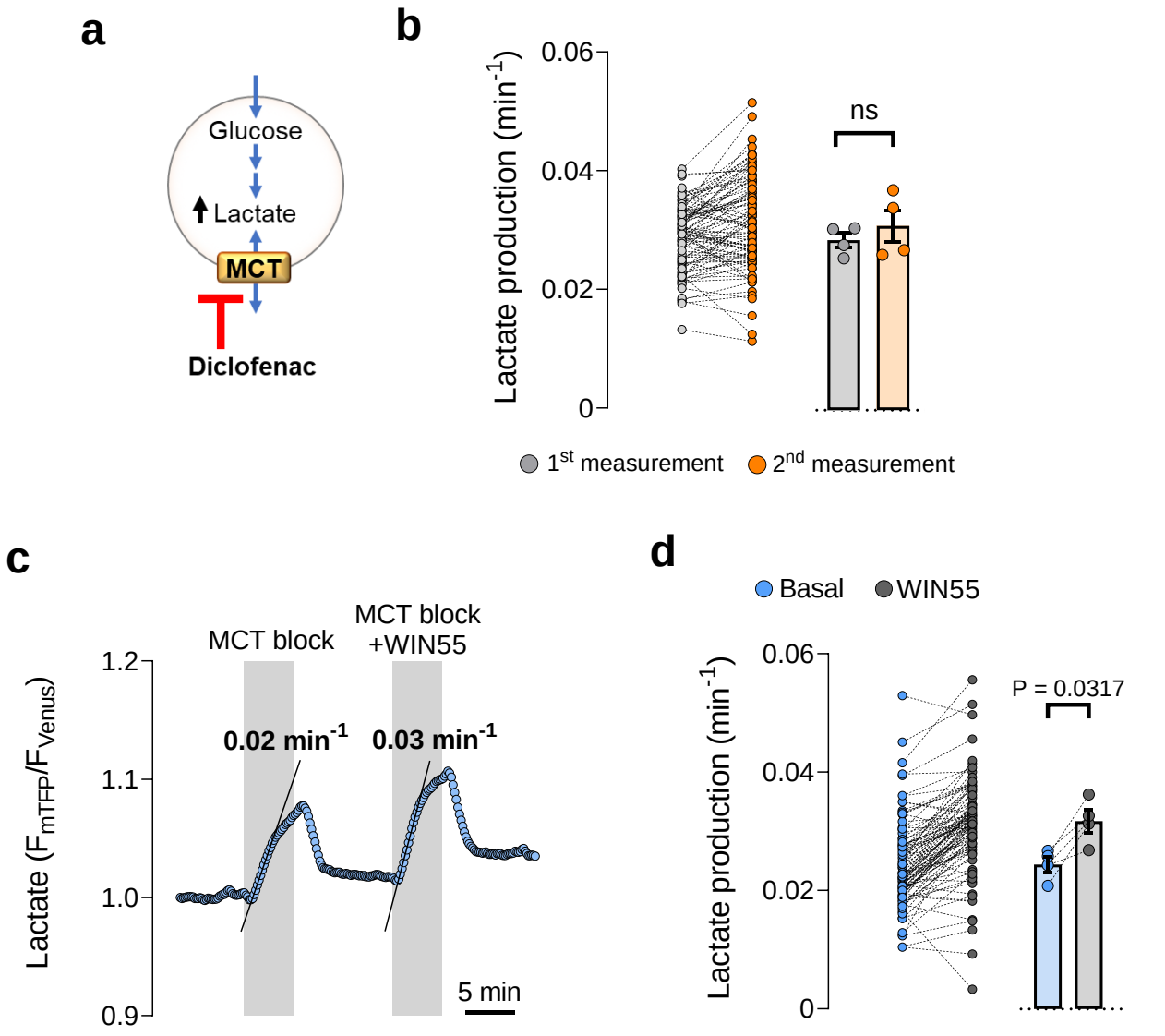

Supplementary Figure 3 – Activation of astroglial CB1 receptors increases lactate production. **a**, Transport stop protocol for measurement of lactate production. Diclofenac is a broad inhibitor of monocarboxylate transporter (MCT) activity. The blockade of MCT causes an intracellular lactate accumulation that is proportional to its rate of production. **b**, Summary of two sequential measurements of basal lactate production with diclofenac. N=4, 95 cells analyzed. **c**, Measurement of lactate production before and during exposure to WIN55 (1 μM). The production rate is indicated with a solid line above the corresponding lactate accumulation. **D**, Summary of the lactate production rates before (pale blue circles) and during exposure to WIN55 (grey circles), computed from experiments similar to panel E. N=4, 102 cells. Data corresponds to representative cell I. Circles in before – after plots correspond to single cells (**b**,**d**). Bars correspond to experiments average (mean±SEM) and circles represent individual experiment average (**b**,**d**). Statistical analysis was performed using a paired two-tailed paired t-test (**b,d**). See Supplementary Table 3 for more details. Source data are provided as a Source Data file.

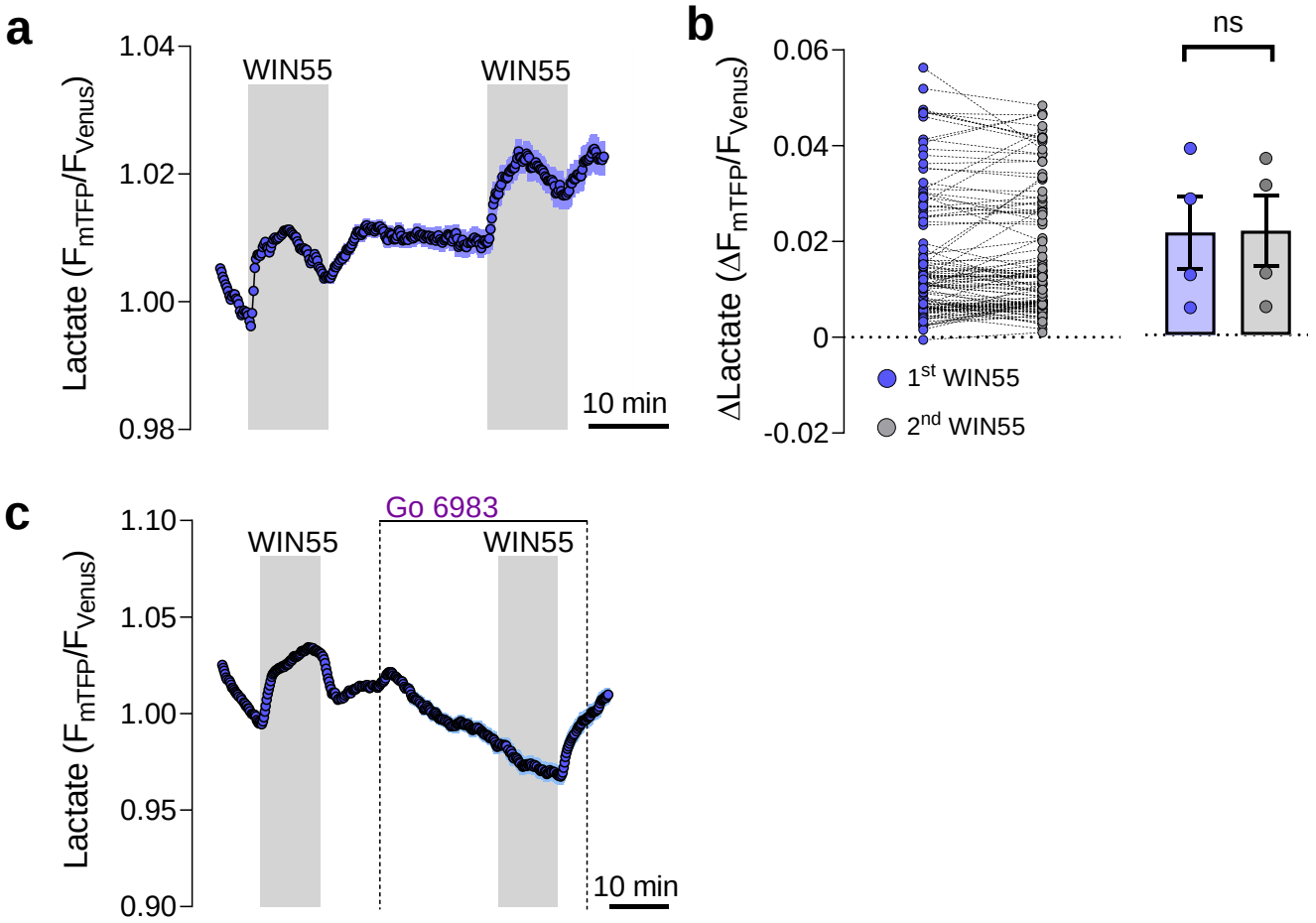

Supplementary Figure 4 – The PKC signaling controls the CB1 receptor-mediated intracellular lactate increase. a, Intracellular lactate measurement during exposure two sequential exposure to WIN55 (1 µM). N=1, 42 cells. **b**, Quantification of lactate change induced by the first (blue) and second (grey) WIN55 exposure. N=4, 114 cells analyzed. **c**, Intracellular lactate measurement during the sequential exposure to WIN55 (1 µM), Go 6983 (5 µM) and WIN55 + Go 6983. N=1, 40 cells. Data corresponds to the average of a single experiment (**a**,**d**). Circles in before – after plots correspond to single cells (**b**). Bars correspond to experiments average (mean±SEM) and circles represent individual experiment average (**b**). Statistical analysis was performed using a paired two-tailed paired t-test (**b**). See Supplementary Table 3 for more details. Source data are provided as a Source Data file.

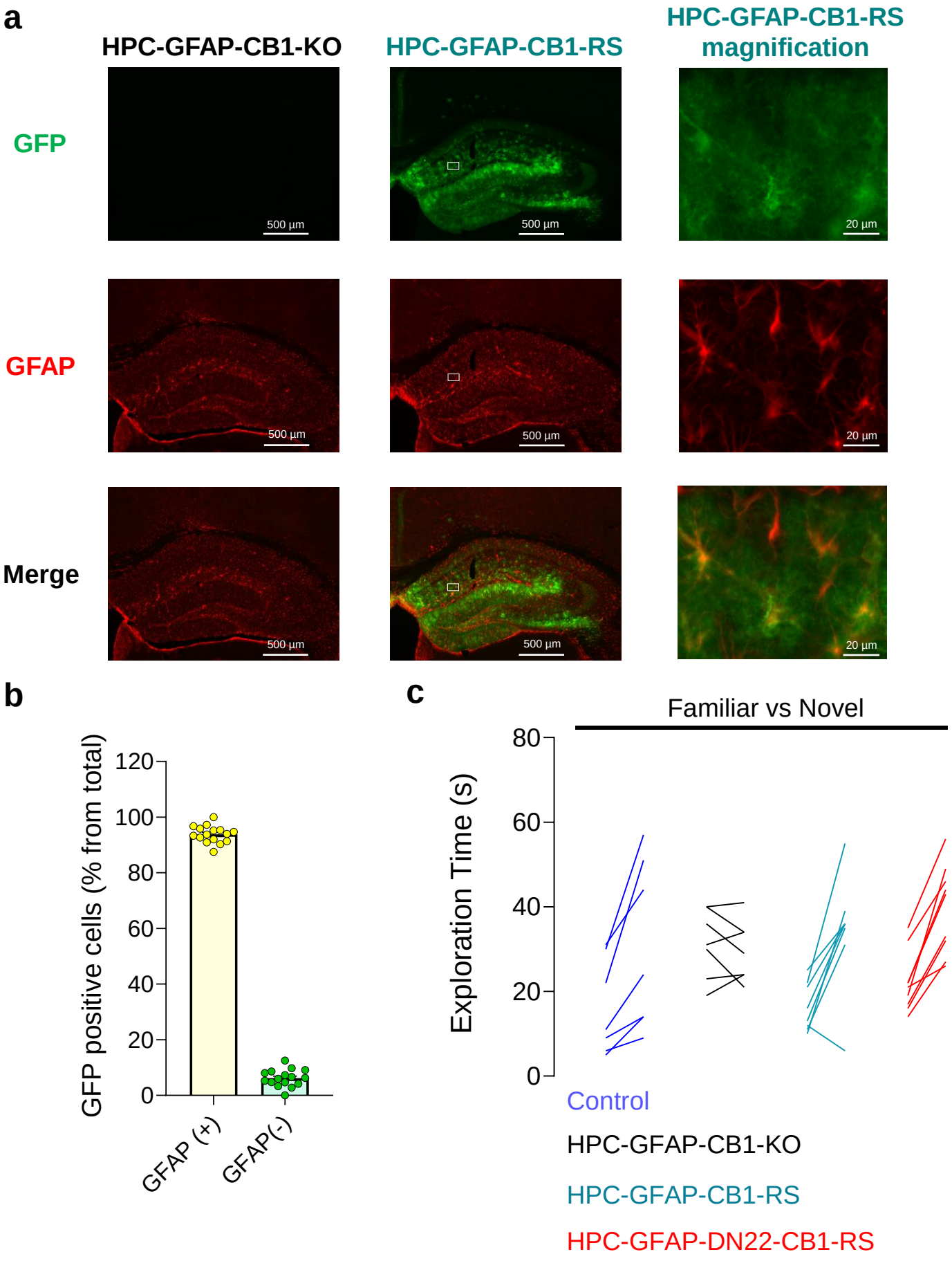
a
HPC-GFAP-CB1-KO
HPC-GFAP-CB1-RS
HPC-GFAP-CB1-RS magnification
GFP
GFAP
Merge
500 µm
20 µm
b
GFP positive cells (% from total)
120
100
80
60
40
20
0
GFAP (+)
GFAP(-)
c
Familiar vs Novel
Exploration Time (s)
80
60
40
20
0
Control
HPC-GFAP-CB1-KO
HPC-GFAP-CB1-RS
HPC-GFAP-DN22-CB1-RS

Supplementary Figure 5 – The mitochondrial localization of CB1 receptors is not necessary for physiological novel object exploration. a, Histological analysis of the expression of CB1-GFP and the astrocyte marker GFAP, in hippocampus sections obtained from HPC-GFAP-CB1-KO and HPC-GFAP-CB1-WT-RS. The white boxes inside the HPC-GFAP-CB1-WT-RS images correspond to the magnification site shown in the third column of images. **b**, Quantification of GFP-positive cells in the CA1 region of the hippocampus of HPC-GFAP-CB1-WT-RS mice. N = 4 mice, 30 – 91 cells analyzed in 4 sections per mice. **c**, Exploration times of familiar versus novel objects in the NOR task, from Control (blue lines), HPC-GFAP-CB1-KO (black lines), HPC-GFAP-CB1-WT-RS (teal lines) and HPC-GFAP- DN22-CB1-RS (red lines) animals, n = 7-9 mice per condition. A single line corresponds to an individual animal. See Supplementary Table 3 for more details. Source data are provided as a Source Data file.

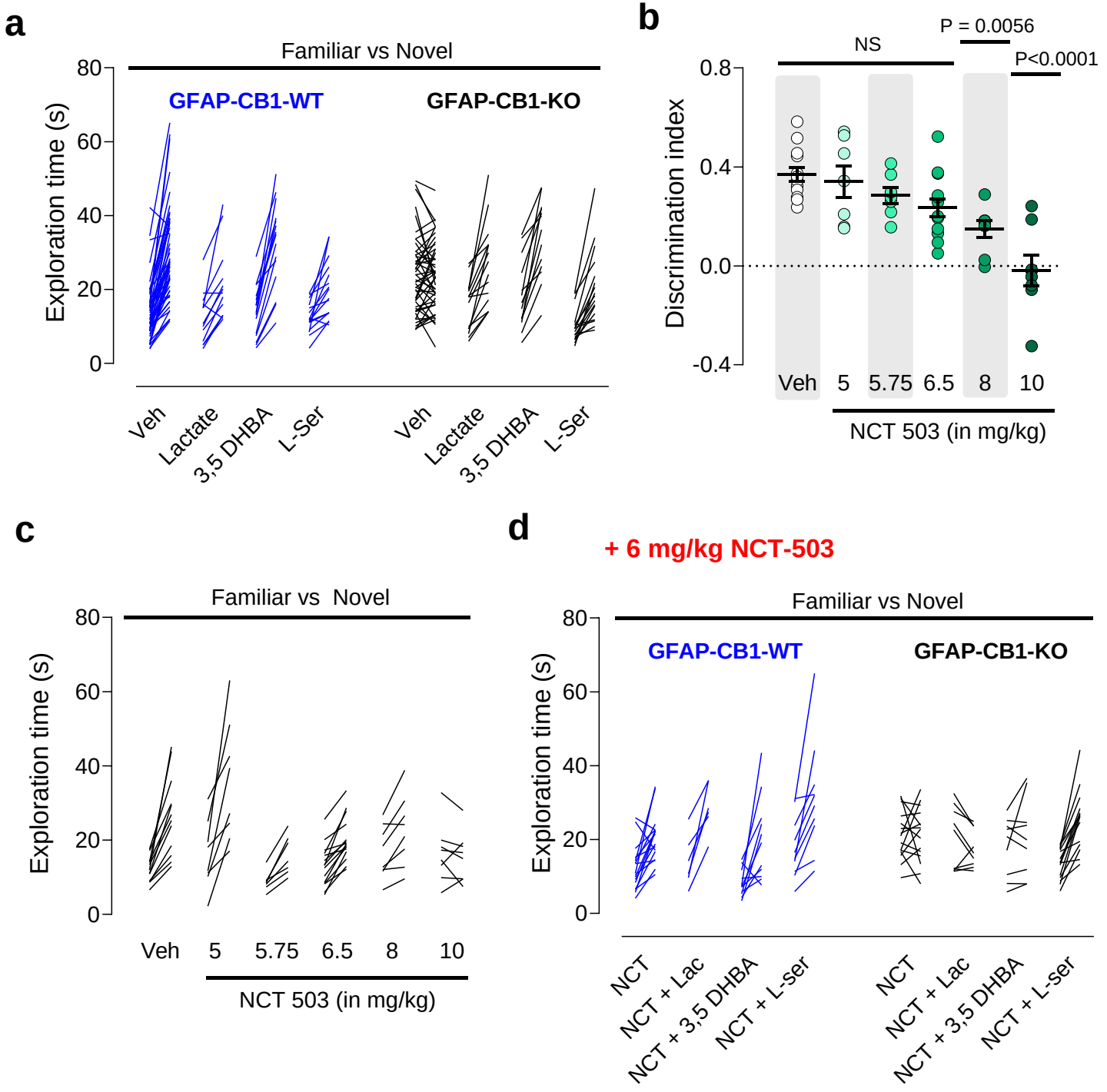

Supplementary Figure 6 – Inhibition of the phosphorylated pathway impairs long-term NOR memory in WT mice and in lactate-treated GFAP-CB1-KO mice. a, Exploration time of familiar versus novel objects in the NOR task of GFAP-CB1-WT (blue lines) and GFAP-CB1-KO mice (black lines) mice, treated either with vehicle (veh), 1 g/kg lactate (Lac) or 0.5 g/kg L-serine (L-Ser), immediately after the acquisition phase. GFAP-CB1-WT, n=13-18 animals. GFAP-CB1-KO, n= 15-23 animals. **b**, NOR performance in wild-type mice treated either with vehicle or incremental doses of NCT-503. N=7-15 mice per condition. **c**, Exploration time of familiar versus novel object in the NOR task of wild-type mice treated either with vehicle or incremental doses of NCT-503. N= 7-15 mice per condition. **d**, Exploration time of familiar versus novel object in the NOR task, of mice treated either

with vehicle + 6 mg/kg NCT-503 (NCT), 1 g/kg lactate + 6 mg/kg NCT-503 (NCT + Lac) or 0.5 g/kg L-serine + 6 mg/kg NCT-503 (NCT + L-Ser), immediately after the acquisition phase. GFAP-CB1-WT mice (blue lines), n=6-12 animals. GFAP-CB1-KO mice (black lines), n= 9-16 animals. A single line corresponds to an individual animal (**a**, **c**, **d**). Data is presented as scatter plot with the line and whisker corresponding to the mean±SEM and circles to individual animals (**b**). Statistical analysis was performed with a One-way ANOVA followed by Tukey's multiple comparison test (**b**). See Supplementary Table 3 for more details. Source data are provided as a Source Data file.

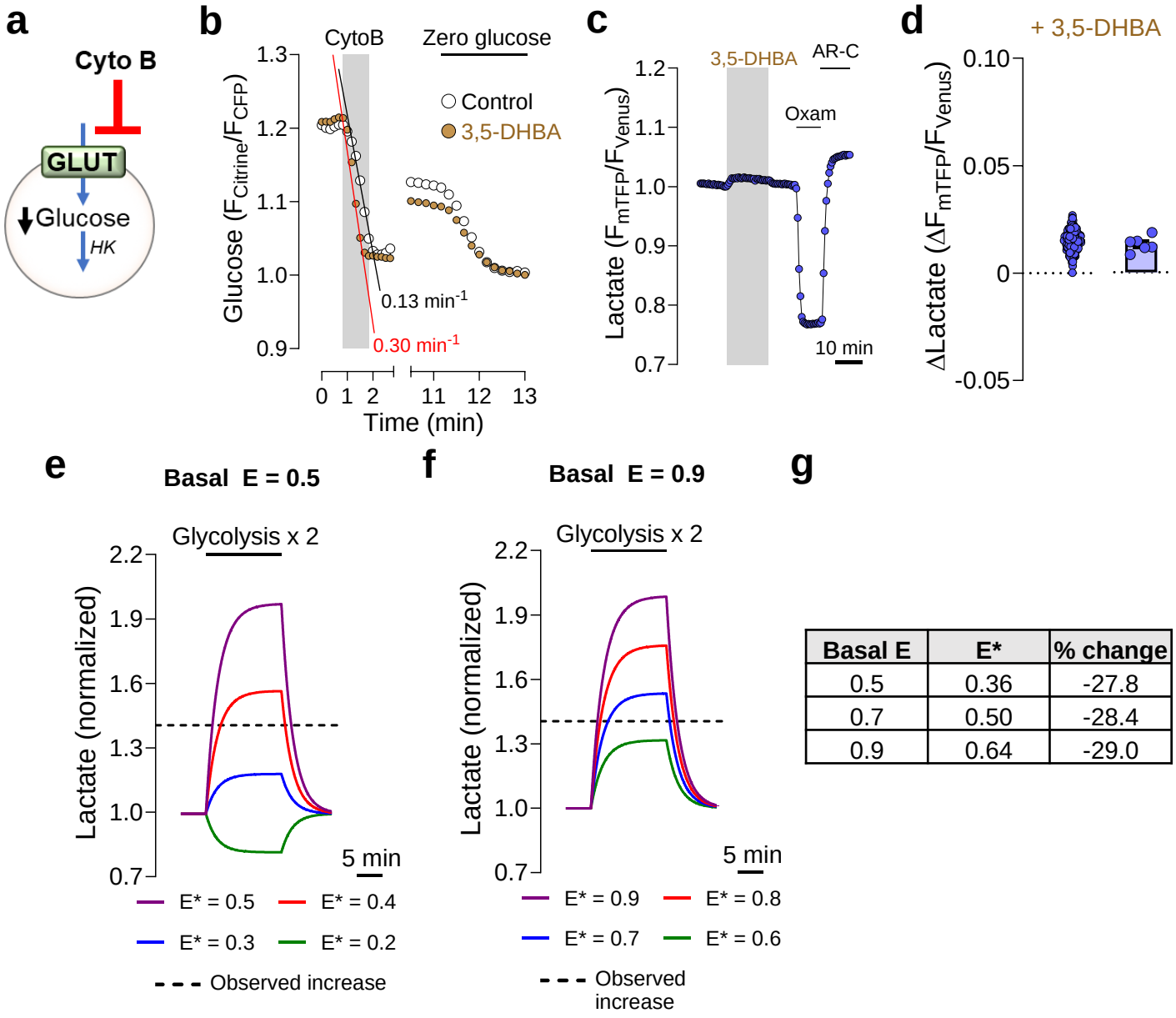

Basal E	E*	% change
0.5	0.36	-27.8
0.7	0.50	-28.4
0.9	0.64	-29.0

Supplementary Figure 7 – Activation of HCA1R promotes a biased glucose metabolism. a, Transport stop protocol for measurement of glucose consumption. Cytochalasin B is an inhibitor of glucose transporter (GLUT) activity. The blockade of GLUT causes an intracellular glucose decrease that is proportional to its rate of consumption by hexokinase (HK), the first enzyme of glycolysis. **b**, Intracellular glucose measurement during exposure to cytochalasin B (CytoB, 20 µM). Astrocytes were treated with 3,5-DHBA (1 mM) for 15 min before exposure to CytoB. **c**, Complete trace of the Fig. 3G intracellular lactate measurement during exposure to 3,5-DHBA, showing the two-point calibration used for transforming the fluorescent ratio to concentration. **d**, Quantification of lactate changes induced by 3,5 DHBA obtained from similar experiments as shown in Fig 3G. N = 6, 222 cells. **e**, Numerical simulation of intracellular lactate concentration (normalized to baseline) with basal E = 0.5, during a two-fold increase in glycolysis. During this stimulation, a decrease in glucose-to-pyruvate/lactate conversion (E*) was simulated. The recorded increase in intracellular lactate

concentration induced by 3,5-DHBA (see methods) is marked by a discontinuous line. **f**, Numerical simulation of intracellular lactate concentration (normalized to baseline) with basal E = 0.9, during a two-fold increase in glycolysis. During this stimulation, a decrease in glucose-to-pyruvate/lactate conversion (E*) was simulated. The recorded increase in intracellular lactate concentration induced by 3,5-DHBA (see methods) is marked by a discontinuous line. **g**, Summary of the E* values required to obtain the observed intracellular lactate concentration induced by 3,5-DHBA for each basal E simulated**.** Data corresponds to representative cells (**b**). Data corresponds to the average (mean+SEM) of representative of experiment (**c**). Circles in scatter plot correspond to individual cells (**d**). Bars correspond to experiments average (mean+SEM) and circles represent experiment average (**d**). Solid line corresponds to a single numerical simulation (**e**,**f**). Source data are provided as a Source Data file.

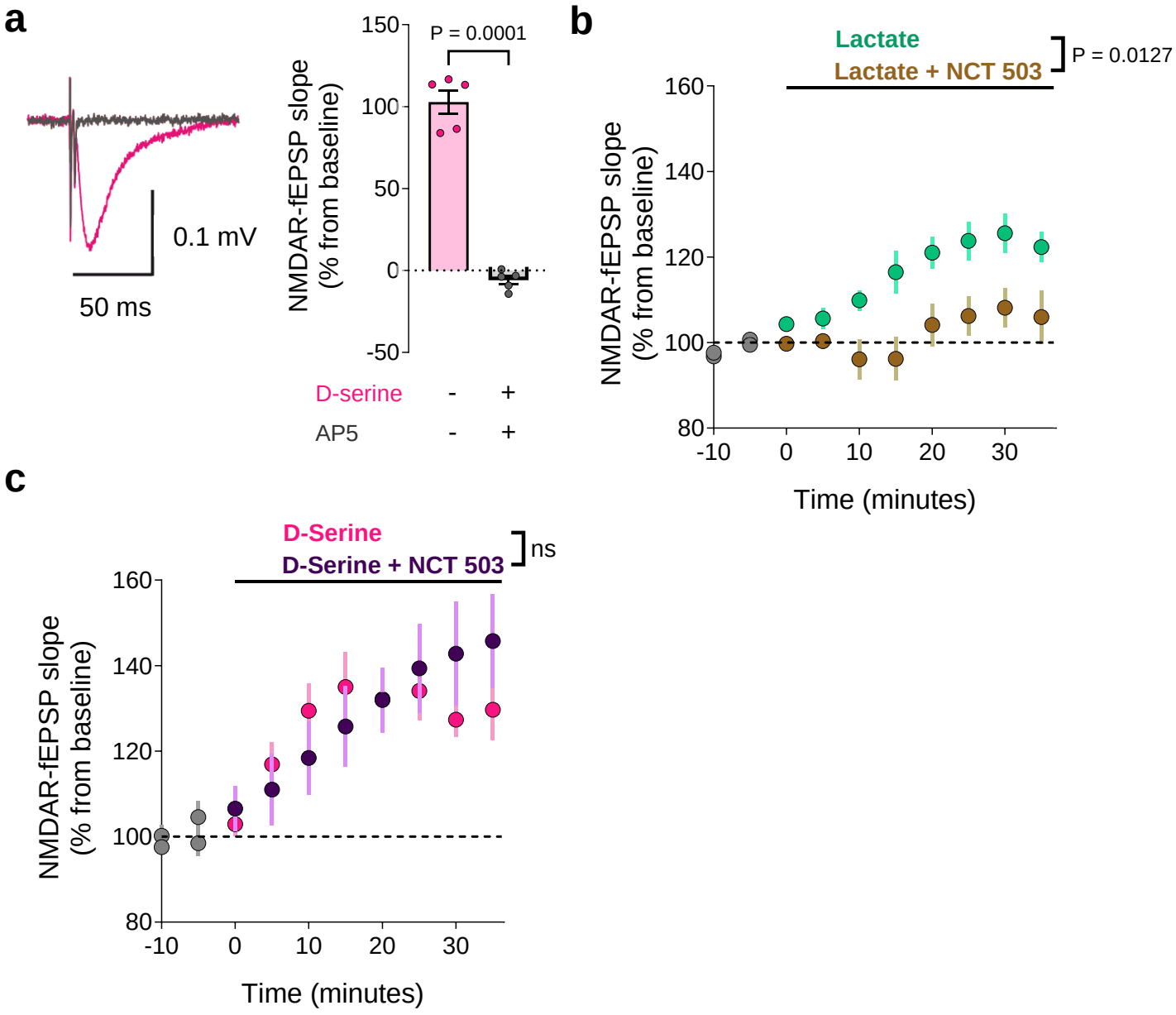

Supplementary Figure 8 – Lactate requires the phosphorylated pathway to potentiate NMDAR function. a, Representative averaged traces from 20 consecutives sweeps evoked in the presence of, before (in magenta) and after bath application of D -AP5 (50 µM) + D -serine (50 µM). Quantification of the NMDAR-fEPSP slopes in presence of D-serine (50 µM), before and after application D-AP5 (50 µM) are shown in the bar plot, n=5. **b**, NMDAR-mediated fEPSP slopes in the presence of lactate (data from Fig. 4A, n=9) and lactate + NCT-503 (data from Fig. 4D, n=6). **c**, NMDAR- fEPSP slopes induced by D-serine (same as Fig. 4A, n=6) and D-serine after NCT-503 preincubation (data from Fig. 4D, n=6). Bars correspond to experiments average (mean±SEM) and circles represent individual experiment average (**a**). Data corresponds to the experiments average and represented as mean±SEM. Data points were averaged every 5 mins (**b**,**c**). Statistical analysis was performed using a two-tailed paired t-test (**a**) and two-way ANOVA (**b**,**c**). See Supplementary Table 3 for more details. Source data are provided as a Source Data file.

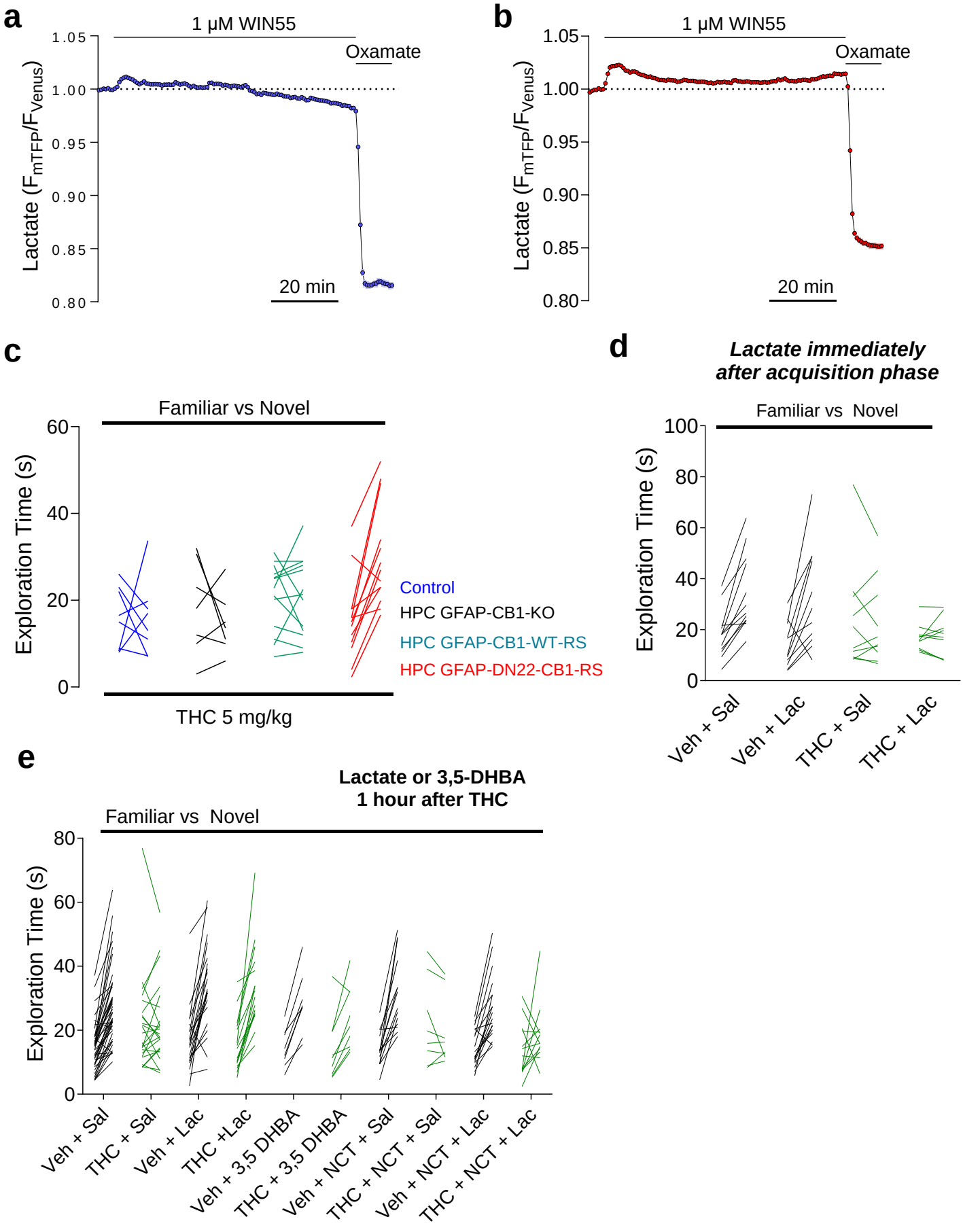
a
1 μM WIN55
Oxamate
Lactate (F_mTFP/F_Venus)
1.05
1.00
0.95
0.90
0.85
0.80
20 min
b
1 μM WIN55
Oxamate
Lactate (F_mTFP/F_Venus)
1.05
1.00
0.95
0.90
0.85
0.80
20 min
c
Familiar vs Novel
Exploration Time (s)
60
40
20
0
Control
HPC GFAP-CB1-KO
HPC GFAP-CB1-WT-RS
HPC GFAP-DN22-CB1-RS
THC 5 mg/kg
d
Lactate immediately after acquisition phase
Familiar vs Novel
Exploration Time (s)
100
80
60
40
20
0
Veh + Sal
Veh + Lac
THC + Sal
THC + Lac
e
Lactate or 3,5-DHBA 1 hour after THC
Familiar vs Novel
Exploration Time (s)
80
60
40
20
0
Veh + Sal
THC + Sal
Veh + Lac
THC +Lac
Veh + 3,5 DHBA
THC + 3,5 DHBA
Veh + NCT + Sal
THC + NCT + Sal
Veh + NCT + Lac
THC + NCT + Lac

Supplementary Figure 9 – Lactate rescues the THC-mediated impairment in novel object exploration via HCAR1 signaling and L-serine production. a, Intracellular lactate imaging in CB1-WT astrocytes exposed to WIN55 (1 μM) during 70 min. After this, cells were exposed to oxamate to deplete lactate levels for biosensor calibration. **b**, Intracellular lactate imaging in DN22-CB1-KI astrocytes exposed to WIN55 (1 μM) during 70 min. After this, cells were exposed to oxamate to deplete lactate levels for biosensor calibration. **c**, Exploration times of familiar versus novel objects in the NOR task, from Control (blue lines), GFAP-CB1-KO (black lines), GFAP-CB1-WT-RS (teal lines) and GFAP- DN22-CB1-RS (red lines) animals treated with THC (5 mg/kg immediately after the acquisition phase. N = 7 – 13 mice per condition. **d**, Exploration time of familiar versus novel objects in the NOR task of mice treated with an IP injection of either vehicle (veh) + saline (sal), vehicle + lactate (lac, 1 g/kg), THC (5 mg/kg) + saline or THC (5 mg/kg) + lactate (1 g/kg), immediately after the acquisition phase. N= 10 – 12 mice per condition. **e**, Exploration time of familiar versus novel objects in the NOR task of mice treated with an IP injection of either vehicle (veh) or THC (5 mg/kg), immediately after the acquisition phase. After 1-hour post-THC treatment, mice were treated with an IP injection of either saline (sal), lactate (lac, 1g/kg), 3,5-DHBA (240 mg/kg), NCT-503 (NCT, 6 mg/kg) + saline or NCT-503 + lactate. N = 8 – 49 mice per condition. Experiments correspond to a representative cell (**a**, **b**). A single line corresponds to an individual animal (**c**, **d**, **e**). See Supplementary Table 3 for more details. Source data are provided as a Source Data file.

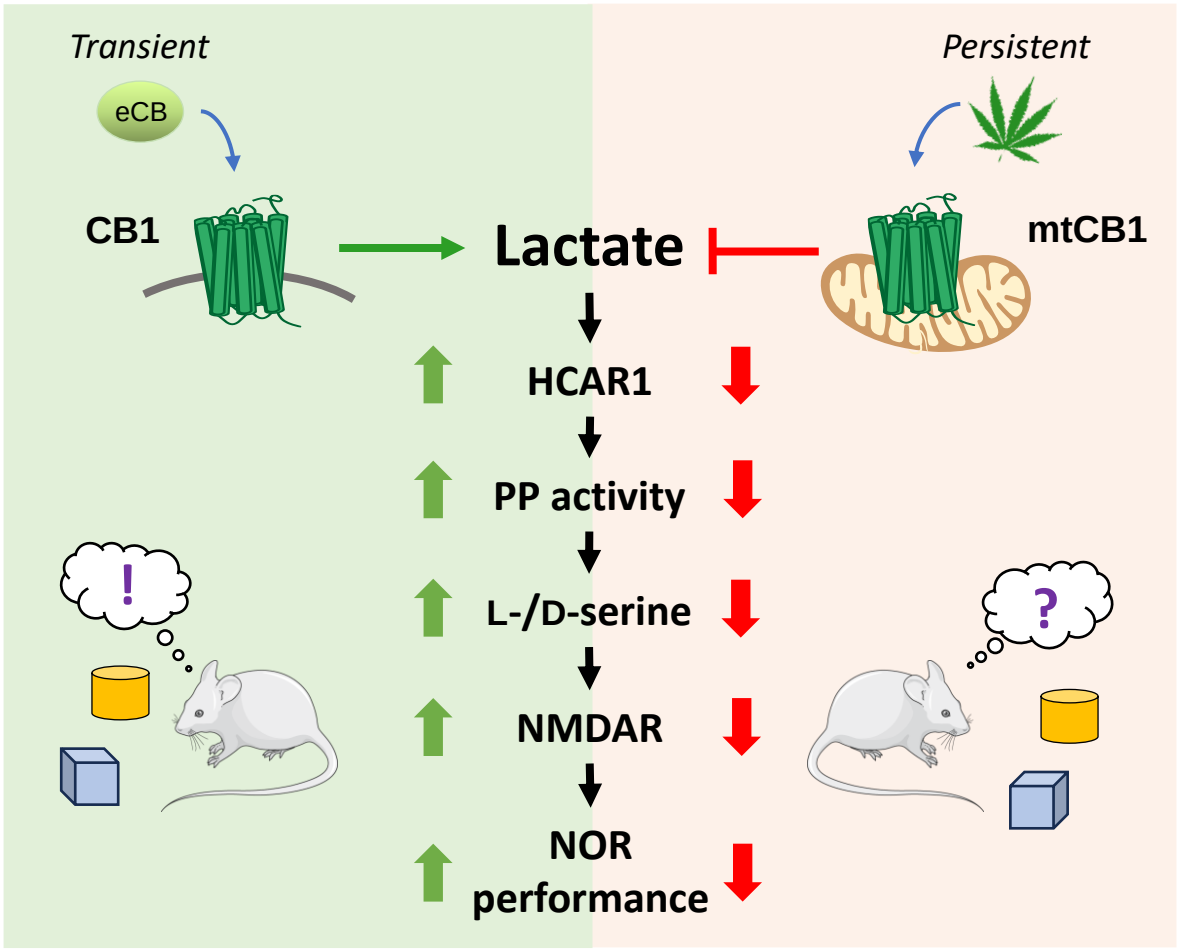

Supplementary Figure 10 – A lactate-dependent shift of glycolysis mediates synaptic and cognitive processes. Lactate promotes cognitive performance via a cascade involving HCAR1 and phosphorylated pathway (PP) activity, thereby increasing L-/D-serine levels and NMDAR activity to allow an adequate NOR memory consolidation. Importantly, whereas transient activation of non-mitochondrial CB1 receptors promote this novel lactate signaling to promote cognitive performance, the persistent activation of mitochondrial CB1 receptors impairs the lactate signaling and disrupt the consolidation of NOR memory via a specular mechanism. The mice cartoon was adapted from a picture provided by Servier Medical Art (https://smart.servier.com/smart_image/mouse-3/), licensed under a Creative Commons Attribution 4.0 Unported License.

Supplementary Table 1.

Details of the double-viral rescue approach to study mtCB1 receptor involvement in NOR performance

Mice	AAV-1*	AAV-2*	Outcome	Mitochondrial Localization of CB1?	Name of used mutant mice
CB1-flox	GFAP-GFP	CAG-DIO-Empty	CB1-WT	yes	**Control**
CB1-flox	GFAP-Cre	CAG-DIO-Empty	CB1-KO in GFAP positive cells	no	**HPC-GFAP-CB1-KO**
CB1-flox	GFAP-Cre	CAG-DIO-CB1-GFP	Re-expression of CB1-WT in GFAP positive cells (CB1 in all subcellular locations)	yes	**HPC-GFAP-CB1-RS**
CB1-flox	GFAP-Cre	CAG-DIO-DN22-CB1-GFP	Re-expression of DN22-CB1 in GFAP positive cells (CB1 excluded from mitochondria)	no	**HPC-GFAP-DN22-CB1-RS**

*Injected into the hippocampus (HPC)

Supplementary Table 2 - Main figures statistics details

Group sizes, statistical tests and P-values (page 1/2)

Figure	Group	N	Mean	SEM	Statistical test	P value	Multiple comparisons (reported in figure)	P value
Fig. 1C	CB1-WT	7	0.0162	0.0029	Kruskal Wallis test	<0.0001	CB1-WT vs. CB1-KO	0.0133
	CB1-KO	7	-0.0005	0.0025			CB1-WT vs. DN22-CB1	>0.9999
	DN22-CB1	6	0.0211	0.0038			CB1-KO vs. DN22-CB1	0.0021
Fig 1F	Sniffers	3	-0.0105	0.0069	One way ANOVA	0.0001	Sniffers vs Sniffers + Astro CB1-WT	0.0004
	Sniffers + Astro CB1-WT	7	0.0959	0.0134			Sniffers vs Sniffers + Astro CB1-KO	0.8163
	Sniffers + Astro CB1-KO	4	0.0022	0.0049			Sniffers + Astro CB1-WT vs Sniffers + Astro CB1-KO	0.0005
Fig. 1I	Basal	4	0.0341	0.005184	Two tailed paired T-test	<0.0001		
	Go 6983	4	-0.01105	0.004554				
Fig. 2B	Control	7	0.306	0.043	One way ANOVA	0.002	Control vs. HPC-GFAP-CB1-KO	0.0066
	HPC-GFAP-CB1-KO	7	-0.024	0.038			Control vs. HPC-GFAP-CB1-RS	>0.9999
	HPC-GFAP-CB1-RS	8	0.306	0.102			Control vs. HPC-GFAP-DN22-CB1-RS	0.9962
	HPC-GFAP-DN22-CB1-RS	9	0.287	0.033			HPC-GFAP-CB1-KO vs. HPC-GFAP-CB1-RS	0.0049
							HPC-GFAP-CB1-KO vs. HPC-GFAP-DN22-CB1-RS	0.0067
							HPC-GFAP-CB1-KO vs. HPC-GFAP-DN22-CB1-RS	0.9957
Fig. 3 B,D	Vehicle : GFAP-CB1-WT	50	0.3637	0.0246	Two way ANOVA		Vehicle:GFAP-CB1-WT vs. Vehicle:GFAP-CB1-KO	<0.0001
	Vehicle : GFAP-CB1-KO	49	0.0005	0.0239	Interaction	<0.0001	Vehicle:GFAP-CB1-WT vs. Lactate:GFAP-CB1-WT	0.9958
	Lactate : GFAP-CB1-WT	13	0.2927	0.0547	Treatment	<0.0001	Vehicle:GFAP-CB1-WT vs. L-Serine:GFAP-CB1-WT	0.2718
	Lactate : GFAP-CB1-KO	15	0.2760	0.0407	Genotype	<0.0001	Vehicle:GFAP-CB1-WT vs. 3,5 DHBA:GFAP-CB1-WT	0.9995
	3,5-DHBA : GFAP-CB1-WT	15	0.4190	0.0331			Vehicle:GFAP-CB1-WT vs. NCT:GFAP-CB1-WT	0.8037
	3,5-DHBA : GFAP-CB1-KO	10	0.3046	0.0440			Vehicle:GFAP-CB1-WT vs. NCT + Lac:GFAP-CB1-WT	>0.9999
	L-serine : GFAP-CB1-WT	16	0.2216	0.0419			Vehicle:GFAP-CB1-WT vs. NCT + L-Serine:GFAP-CB1-WT	0.9501
	L-serine : GFAP-CB1-KO	17	0.3246	0.0403			Vehicle:GFAP-CB1-WT vs. NCT + 3,5-DHBA:GFAP-CB1-WT	>0.9999
	Vehicle : GFAP-CB1-WT : NCT-503	17	0.2631	0.0532			Vehicle:GFAP-CB1-KO vs. Lactate:GFAP-CB1-KO	<0.0001
	Vehicle : GFAP-CB1-KO : NCT-503	14	-0.0097	0.0533			Vehicle:GFAP-CB1-KO vs. L-Serine:GFAP-CB1-KO	<0.0001
	Lactate : GFAP-CB1-WT : NCT-503	6	0.3656	0.0701			Vehicle:GFAP-CB1-KO vs. 3,5 DHBA:GFAP-CB1-KO	0.0001
	Lactate : GFAP-CB1-KO : NCT-503	9	-0.0484	0.0467			Vehicle:GFAP-CB1-KO vs. NCT:GFAP-CB1-KO	>0.9999
	3,5-DHBA : GFAP-CB1-WT : NCT-503	9	0.2565	0.0480			Lactate:GFAP-CB1-WT vs. Lactate:GFAP-CB1-KO	>0.9999
	3,5-DHBA : GFAP-CB1-KO : NCT-503	9	0.0599	0.0460			Lactate:GFAP-CB1-WT vs. L-Serine:GFAP-CB1-WT	0.9995
	L-serine : GFAP-CB1-WT : NCT-503	11	0.3655	0.0926			Lactate:GFAP-CB1-WT vs. 3,5 DHBA:GFAP-CB1-WT	0.8778
	L-serine : GFAP-CB1-KO : NCT-503	16	0.3019	0.0354			Lactate:GFAP-CB1-WT vs. NCT + Lac:GFAP-CB1-WT	>0.9999
							L-Serine:GFAP-CB1-WT vs. L-Serine:GFAP-CB1-KO	0.951
							L-Serine:GFAP-CB1-KO vs. 3,5 DHBA:GFAP-CB1-KO	>0.9999
							3,5 DHBA:GFAP-CB1-WT vs. 3,5 DHBA:GFAP-CB1-KO	0.9689
							3,5 DHBA:GFAP-CB1-WT vs. NCT:GFAP-CB1-WT	0.4767
							3,5 DHBA:GFAP-CB1-WT vs. NCT + 3,5-DHBA:GFAP-CB1-WT	>0.9999
							NCT:GFAP-CB1-WT vs. NCT:GFAP-CB1-KO	0.0026
							NCT + Lac:GFAP-CB1-WT vs. NCT + Lac:GFAP-CB1-KO	0.0013
							NCT + L-Serine:GFAP-CB1-WT vs. NCT + L-Serine:GFAP-CB1-KO	>0.9999
							NCT + 3,5-DHBA:GFAP-CB1-WT vs. NCT + 3,5-DHBA:GFAP-CB1-KO	0.0134
Fig 3E	Control	63 cells	0.1014	0.0086	Mann-Whitney	<0.0001		
	3,5-DHBA	48 cells	0.2011	0.0148				
Fig. 4A	Lactate	8	124	11.86	Two-tailed unpaired T-test	0.5927		
	D-serine	5	127.7	12.25				
Fig. 4B	Lactate	8	0.09335	0.01583	Two-tailed unpaired T-test	0.0032		
	D-Serine	5	0.294	0.06443				
Fig. 4C	baseline	6	100.1	0.1091	Two-tailed paired T-test	0.6782		
	Lactate	6	102.1	4.389				
Fig. 4D	Lactate + NCT-503	6	111.4	6.615	Two-tailed unpaired T-test	0.0212		
	D-Serine + NCT-503	6	138.8	7.576				
	baseline (NCT-503)	6	99.92	0.1241	Two-tailed paired T-test	0.143		
	Lactate + NCT-503	6	111.4	6.615				
Fig. 4F	Baseline	6	101	0.747	Two-tailed paired T-test	0.0096		
	3,5-DHBA	6	128.8	6.888				
	Baseline	8	100.6	0.8498	Two-tailed paired T-test	0.4576		
	D-serine	8	104.2	4.463				

Supplementary Table 2 - Main figures statistics details

Group sizes, statistical tests and P-values (page 2/2)

Fig. 5A	5 min post WIN55	11	0.0149	0.0024	**Mixed-effects model**	<0.0001	baseline vs. 5 min	0.0277
	10 min post WIN55	4	0.0085	0.0045			baseline vs. 10 min	0.3801
	20 min post WIN55	4	0.0037	0.0042			baseline vs. 20 min	0.9626
	30 min post WIN55	4	-0.0001	0.0049			baseline vs. 30 min	>0.9999
	40 min post WIN55	4	-0.0042	0.0040			baseline vs. 40 min	0.9315
	50 min post WIN55	4	-0.0110	0.0049			baseline vs. 50 min	0.1578
	60 min post WIN55	4	-0.0179	0.0078			baseline vs. 60 min	0.007
	70 min post WIN55	4	-0.0264	0.0090			baseline vs. 70 min	<0.0001
Fig. 5B	5 min post WIN55	10	0.0242	0.0030	**Mixed-effects model**	0.001	baseline vs. 5 min	0.0002
	10 min post WIN55	4	0.0245	0.0069			baseline vs. 10 min	0.0013
	20 min post WIN55	4	0.0202	0.0082			baseline vs. 20 min	0.0087
	30 min post WIN55	4	0.0165	0.0072			baseline vs. 30 min	0.0399
	40 min post WIN55	4	0.0155	0.0060			baseline vs. 40 min	0.0573
	50 min post WIN55	4	0.0125	0.0029			baseline vs. 50 min	0.1711
	60 min post WIN55	4	0.0095	0.0011			baseline vs. 60 min	0.4141
	70 min post WIN55	4	0.0081	0.0034			baseline vs. 70 min	0.5788
Fig. 5C	Control	8	-0.0226	0.1276	**One way ANOVA**	0.002	Control vs. HPC-GFAP-CB1-KO	0.9981
	HPC-GFAP-CB1-KO	7	-0.0466	0.1176			Control vs. HPC-GFAP-CB1-RS	0.9991
	HPC-GFAP-CB1-RS	13	-0.0062	0.0545			Control vs. HPC-GFAP-DN22-CB1-RS	0.0158
	HPC-GFAP-DN22-CB1-RS	13	0.3594	0.0679			HPC-GFAP-CB1-KO vs. HPC-GFAP-CB1-RS	0.9884
							HPC-GFAP-CB1-KO vs. HPC-GFAP-DN22-CB1-RS	0.0136
							HPC-GFAP-CB1-KO vs. HPC-GFAP-DN22-CB1-RS	0.0071
Fig 5D	Vehicle : Saline	12	0.3246	0.0444	**Two way ANOVA**		Saline:Vehicle vs. Saline:THC	0.0003
	THC : Saline	11	-0.0178	0.0610	Interaction	0.505	Saline:Vehicle vs. Lactate:Vehicle	0.7752
	Vehicle : Lactate	10	0.3953	0.0620	Lactate	0.5317	Saline:Vehicle vs. Lactate:THC	0.0003
	THC : Lactate	10	-0.0200	0.0484	THC	<0.0001	Saline:THC vs. Lactate:Vehicle	<0.0001
							Saline:THC vs. Lactate:THC	>0.9999
							Lactate:Vehicle vs. Lactate:THC	<0.0001
Fig. 5E	Vehicle : Saline	42	0.305362	0.027283	**Two way ANOVA**		Saline + Vehicle vs. Saline + THC	<0.0001
	THC : Saline	24	0.015965	0.04061	Interaction	0.0001	Saline + Vehicle vs. Lactate 1h after + Vehicle	0.9999
	Vehicle : Lactate	21	0.339832	0.051617	Treatment 2	<0.0001	Saline + Vehicle vs. Lactate 1h after + THC	0.9011
	THC : Lactate	23	0.387984	0.051963	THC	<0.0001	Saline + Vehicle vs. 3,5 DHBA 1h after + Vehicle	>0.9999
	Vehicle : 3,5-DHBA	8	0.339324	0.03525			Saline + Vehicle vs. 3,5 DHBA 1h after + THC	>0.9999
	THC : 3,5-DHBA	9	0.306085	0.062923			Saline + Vehicle vs. NCT + Vehicle	0.982
	Vehicle : Saline : NCT-503	14	0.380169	0.049633			Saline + Vehicle vs. NCT + THC	0.0016
	THC : Saline : NCT-503	12	0.006681	0.055404			Saline + THC vs. Lactate 1h after + THC	<0.0001
	Vehicle : Lactate : NCT-503	18	0.300849	0.042664			Saline + THC vs. 3,5 DHBA 1h after + Vehicle	0.0119
	THC : Lactate : NCT-503	17	0.054124	0.083171			Saline + THC vs. 3,5 DHBA 1h after + THC	0.0252
							Saline + THC vs. NCT + Vehicle	<0.0001
							Saline + THC vs. NCT + THC	>0.9999
							Saline + THC vs. Lactate + NCT + THC	>0.9999
							Lactate 1h after + Vehicle vs. Lactate 1h after + THC	0.9992
							Lactate 1h after + Vehicle vs. Lactate + NCT + THC	0.003
							3,5 DHBA 1h after + Vehicle vs. 3,5 DHBA 1h after + THC	>0.9999
							Lactate + NCT + Vehicle vs. Lactate + NCT + THC	0.0302

Supplementary Table 3 - Supplementary figures statistics details

Group sizes, statistical tests and P-values

Figure	Group	N	Mean	SEM	Statistical test	P value	Multiple comparisons (reported in figure)	P value
Ext. data Fig 1B	Vehicle	3	0.7325	0.01123	**Two-tailed unpaired T-test**	<0.0001		
	WIN55	3	0.5498	0.02122				
Ext. data Fig 1D	Baseline (BL)	3	0.9929	0.002431	**Two-tailed paired T-test**	<0.0001		
	WIN55	3	1.032	0.001816				
Ext. data Fig 2B	CB1-WT	4	0.4798	0.05392	**Kruskal-Wallis test**	0.6298	CB1-WT vs. CB1-KO	0.9804
	CB1-KO	4	0.5483	0.03634			CB1-WT vs. DN22-CB1	>0.9999
	DN22-WT	4	0.5541	0.0473			CB1-KO vs. DN22-CB1	>0.9999
Ext. data Fig 2C	CB1-WT	4	0.06298	0.01233	**One way ANOVA**	0.4612	CB1-WT vs. CB1-KO	0.449
	CB1-KO	4	0.04552	0.009156			CB1-WT vs. DN22-CB1	0.6554
	DN22-WT	4	0.05058	0.007127			CB1-KO vs. DN22-CB1	0.9295
Ext. data Fig 2D	CB1-WT	7	0.0385	0.004412	**One way ANOVA**	0.3815	CB1-WT vs. CB1-KO	0.3496
	CB1-KO	7	0.02675	0.006981			CB1-WT vs. DN22-CB1	0.7466
	DN22-WT	6	0.0322	0.00623			CB1-KO vs. DN22-CB1	0.8022
Ext. data Fig 3B	First measurement	4	0.02854	0.001203	**Two-tailed paired T-test**	0.2564		
	Second measurement	4	0.03095	0.002664				
Ext. data Fig 3D	Basal	4	0.02441	0.0013	**Two-tailed paired T-test**	0.0317		
	WIN55	4	0.03174	0.001944				
Ext. data Fig 4B	First measurement	4	0.02143	0.007549	**Two-tailed paired T-test**	0.391		
	Second measurement	4	0.02148	0.007517				
Ext. data Fig 5B	GFP (+) - GFAP (+)	4	93.81	0.762				
	GFP (+) - GFAP (-)	4	6.195	0.762				
Ext. data Fig 6B	Vehicle	13	0.3688	0.02855	**One way ANOVA**	<0.0001	Vehicle vs. 5 mg/kg	0.9973
	5 mg/kg NCT-503	7	0.3407	0.06452			Vehicle vs. 5.75 mg/kg	0.7351
	5.75 mg/kg NCT-503	7	0.2842	0.03302			Vehicle vs. 6.5 mg/kg	0.0911
	6.5mg/kg NCT-503	15	0.2353	0.03493			Vehicle vs. 8 mg/kg	0.0056
	8 mg/kg NCT-503	8	0.1494	0.03349			Vehicle vs. 10 mg/kg	<0.0001
	10 mg/kg NCT-503	8	-0.01882	0.06185			5 mg/kg vs. 5.75 mg/kg	0.964
							5 mg/kg vs. 6.5 mg/kg	0.4935
							5 mg/kg vs. 8 mg/kg	0.0667
							5 mg/kg vs. 10 mg/kg	<0.0001
							5.75 mg/kg vs. 6.5 mg/kg	0.9622
							5.75 mg/kg vs. 8 mg/kg	0.3556
							5.75 mg/kg vs. 10 mg/kg	0.0005
							6.5 mg/kg vs. 8 mg/kg	0.6613
							6.5 mg/kg vs. 10 mg/kg	0.0006
							8 mg/kg vs. 10 mg/kg	0.1195
Ext. data Fig 7D	3,5-DHBA	4	0.01303	0.001426				
Ext. data Fig 8A	D-serine	5	102.7	7.238	**Two-tailed paired T-test**	0.0001		
	D-serine + D-AP5	5	-5.945	2.604				
Ext. data Fig 8B		**N**			**Two way ANOVA**			
	Lactate	9			Time x Treatment	0.0007		
	Lactate + NCT-503	5			Time	<0.0001		
					Treatment	0.0127		
Ext. data Fig 8C		**N**			**Two way ANOVA**	**P value**		
	D-serine	6			Time x Treatment	0.0604		
	D-serine + NCT-503	4			Time	<0.0001		
					Treatment	0.6915		